SILAC-Based Quantitative Proteomics Identifies Multifactorial Mechanism of Oxaliplatin Resistance in Pancreatic Cancer Cells

Young Eun Kim[1,2,§], Eun-Kyung Kim[3, §], Min-Jeong Song[3], Tae-Young Kim[2], Ho Hee Jang [3,*]

Dukjin Kang[1,*]

[1]Center for Bioanalysis, Division of Chemical and Medical Metrology, Korea Research Institute of Standards and Science, Daejeon 34113, Republic of Korea

[2]School of Earth Sciences and Environmental Engineering, Gwangju Institute of Science and Technology, Gwangju 61005, Republic of Korea

[3]Department of Biochemistry, College of Medicine, Gachon University, Incheon 21999, Republic of Korea

[§]Both authors contributed equally to this study

[*]Corresponding author: **Dukjin Kang**, Phone: +82-42-868-5700, Fax: +82-42-868-5801, E-mail: djkang@kriss.re.kr, and **Ho Hee Jang**, Phone: +82-32-899-6317, Fax: +82-32-899-6318, E-mail: hhjang@gachon.ac.kr

Running title: Proteomic profiling of oxaliplatin-resistant PANC-1 cells

Abbreviations

SILAC, stable isotope labelling by amino acids in cell culture

2D-nLC-MS/MS, two-dimensional nanoflow liquid chromatography-tandem mass spectrometry

PPI, protein-protein interaction

MARCKS, myristoylated alanine-rich C-kinase substrate

WLS, wntless homolog protein

PI3K/AKT, phosphatidylinositol 3-kinase/protein kinase B

qRT-PCR, real-time quantitative reverse transcription-PCR

siRNA, short interfering RNA

Keywords: quantitative proteomics, SILAC, pancreatic cancer, drug resistance, oxaliplatin

Abstract

Oxaliplatin is a commonly used chemotherapeutic drug for the treatment of pancreatic cancer. Understanding the cellular mechanisms of oxaliplatin resistance is important for developing new strategies to overcome drug resistance in pancreatic cancer. In this study, we performed a stable isotope labelling by amino acids in cell culture (SILAC)-based quantitative proteomic analysis of oxaliplatin-resistant and sensitive pancreatic cancer PANC-1 cells. We identified 107 proteins whose expression levels changed between oxaliplatin-resistant and sensitive cells, which were involved in multiple biological processes, including DNA repair, drug response, apoptotic signalling, and the type 1 interferon signalling pathway. Notably, myristoylated alanine-rich C-kinase substrate (MARCKS) and wntless homolog protein (WLS) were upregulated in oxaliplatin-resistant cells compared to sensitive cells, as confirmed by qRT-PCR and Western blot analysis. We further demonstrated the activation of AKT and β-catenin signalling (downstream targets of MARCKS and WLS, respectively) in oxaliplatin-resistant PANC-1 cells. Additionally, we show that the siRNA-mediated suppression of both MARCKS and WLS enhanced oxaliplatin sensitivity in oxaliplatin-resistant PANC-1 cells. Taken together, our results provide insights into multiple mechanisms of oxaliplatin resistance in pancreatic cancer cells and reveal that MARCKS and WLS might be involved in the chemotherapeutic resistance in pancreatic cancer.

Introduction

Pancreatic cancer is one of the most lethal cancers, with the five-year survival rate of 8%, the lowest survival rate among other common types of cancer (1). Despite recent advances in cancer therapeutics, pancreatic cancer still has a poor prognosis, mainly due to a lack of its distinctive symptoms in early stages. In addition, either the spread of pancreatic cancer to

other organs in the abdomen or its chemoresistance during chemotherapy can occur readily in early stages (2, 3).

Oxaliplatin is a platinum-based chemotherapy drug used in the treatment of various types of cancers, including pancreatic, colorectal, and gastric cancers (4-6). The combination of oxaliplatin with other chemotherapy drugs (5-FU, leucovorin, and irinotecan) is one of the standard regimens in first-line treatment for pancreatic cancer (7). Similar to other platinum drugs, oxaliplatin is known to cause DNA damage by the formation of platinum-DNA adducts, resulting in cell toxicity and death (8, 9). Although the use of oxaliplatin is effective in the treatment of cancers, acquired resistance to oxaliplatin often occurs in patients, which leads to therapeutic failures. Many studies have reported the several different mechanisms of resistance to oxaliplatin in the acquired oxaliplatin-resistant cancer cell lines (9-12), which include the regulation of cellular transport and detoxification (10), the enhancement of DNA repair system (12), and the activation of NF-kB signalling (11). However, understanding of multiple mechanisms for acquired oxaliplatin resistance remains a challenge in pancreatic cancer treatments.

Mass spectrometry-based proteomics has become a powerful tool to explore multiple mechanisms of chemoresistance in cancer cells, which allows the global identification and quantification of proteins associated with drug resistance (13-15). For example, an earlier study has reported the comparative proteomic profiling between oxaliplatin sensitive and resistant human colorectal cancer cells (15). These authors detected down-regulation of pyruvate kinase M2 (PK-M2) in oxaliplatin resistant cells and further demonstrated an inverse relationship between PK-M2 expression and oxaliplatin resistance in patients with colorectal cancer.

The aim of this study is to investigate the global proteomic changes associated with

acquired oxaliplatin resistance in pancreatic cancer cells. We established oxaliplatin-resistant PANC-1 cells by stepwise exposure to increasing concentration of oxaliplatin. A stable isotope labelling by amino acids in cell culture (SILAC)-based quantitative proteomics analysis of oxaliplatin sensitive and resistant PANC-1 (PANC-1R) cells was performed using two-dimensional nanoflow liquid chromatography-tandem mass spectrometry (2D-nLC-MS/MS). A number of proteins involved in DNA repair, drug response, apoptosis signalling, and type 1 interferon signalling pathway were significantly changed in PANC-1R cells compared to sensitive cells. Also, we identified myristoylated alanine-rich C-kinase substrate (MARCKS) and wntless homolog protein (WLS) as highly upregulated proteins in PANC-1 R cells, and validated these using qRT-PCR and Western blotting. Finally, we then explored the roles of MARCKS and WLS in oxaliplatin resistance using siRNA silencing.

Experimental procedures

Experimental Design and Statistical Rationale

To perform quantitative proteomic analysis, the human pancreatic cancer PANC-1 cells and oxaliplatin-resistant PANC-1 (PANC-1R) cells were metabolically labelled with the heavy amino acids ($^{13}C_6$-Arg and $^{15}N_2{}^{13}C_6$-Lys) for SILAC-Heavy and their light counterparts ($^{12}C_6$-Arg and $^{14}N_2{}^{12}C_6$-Lys) for SILAC-Light, respectively. SILAC-labelled PANC-1 (heavy) and PANC-1R (light) cells were used for proteomic analysis. The proteomic dataset was obtained from three biological replicates with two technical replicates using on-line 2D-LC-MS/MS. A total of six datasets were obtained, each consisting of 12 MS raw data files. MS raw data were processed using MaxQuant search engine 1.6.1.0. To perform appropriate statistical analysis, we considered only proteins that were quantified at least three times in six datasets.

Student's t-test was performed using the Perseus software 1.5.8.5. P-values less than 0.05 were considered statistically significant. All data showed a normal distribution and linear correlation between replicates (see Result section). For a detailed description of MS data processing and statistical analysis, see the data analysis in the experimental procedures sections.

Establishment of an Oxaliplatin-Resistant Pancreatic Cancer Cell Line

The human pancreatic cancer cell line, PANC-1, was obtained from the Korean Cell Lines Bank (KCLB, Seoul, Korea) and cultured in Dulbecco's Modified Eagle's Medium (DMEM, Capricorn Scientific GmbH, Germany) with 100 units/mL penicillin, 100 µg/mL streptomycin, and 10% fetal bovine serum (FBS) at 37°C with 5% CO_2 in a humidified atmosphere. Anticancer-drug resistant PANC-1 cells were established by means of increasing concentrations of oxaliplatin, as previously described (16857785, 27910856, 23349823). Oxaliplatin (O9512) was purchased from Sigma-Aldrich. To establish a stable pancreatic cancer cell line chronically resistant to oxaliplatin, the PANC-1 cells were cultured at a starting concentration of 20 µg/ml oxaliplatin for 48 h. When the surviving population of PANC-1 cells became 80% confluent, the cells were sub-cultured twice. The concentration of oxaliplatin in the surviving PANC-1 cells was exposed to a stepwise increase in the same manner to 40 µg/ml, and finally to a concentration of 80 µg/ml. The surviving PANC-1 cells with final treatment of oxaliplatin was named PANC-1R. The sensitivity of parental PANC-1 and oxaliplatin-resistant PANC-1R cells to oxaliplatin was determined by cell viability assay analyzed by treatment for 48 h with different concentrations of oxaliplatin.

Cell Viability Assay

Cells were seeded in 96-well plates at a density of 1×10^4 cells/well. Oxaliplatin was treated for 48 h at 37°C with 5% CO_2 in a humidified atmosphere. of Ez-cytox (10 μl/well, Dogen bio, Seoul, South Korea) was incubated at 37°C for 3 h. To measure the number of viable cells, the absorbance of each well was detected at 450 nm using an Epoch-2 microplate reader (BioTek, Winooski, VT, USA). The assays were performed in triplicate.

Colony Forming Assay

Equal numbers of PANC-1 or PANC-1R cells (1,000/well) were seeded into 6-well plates and cultured for 2 weeks in the medium. After washing with phosphate-buffered saline (PBS), the cells were fixed with 4% paraformaldehyde for 30 min and stained with 0.1% crystal violet (C0775, Sigma-Aldrich) for 30 min at room temperature. The number of colonies was counted under a light microscope.

Stable Isotope Labelling with Amino Acids in Cell Culture (SILAC)

PANC-1cells were cultured in SILAC DMEM medium (Welgene, Daegu, Korea) with dialyzed FBS (Gibco, USA) containing heavy 0.798 mM lysine and 0.398 mM arginine. Heavy lysine (1G: CLM-265-H-1) and arginine (1G: CNLM-291-H-1) were purchased from Cambridge Isotope Laboratories (CIL, USA). PANC-1R cells were grown in light SILAC growth medium (DMEM, Capricorn Scientific GmbH, Germany) with dialyzed FBS (Gibco, USA). All cells were maintained at 37°C in humidified air containing 5% CO_2. To validate labelling efficiency for full incorporation of heavy amino acid labels in all proteins, cells were cultured for seven passages and checked reached > 95% by LC-MS/MS analysis.

Sample Preparation for Proteomic Analysis

PANC-1 and PANC-1R cells were suspended with cell lysis buffer (8 M urea, 50 mM Tris-HCl pH 8.0, 75 mM NaCl, and a cocktail of protease inhibitors) and sonicated with ten 3-s pulses (2-s pause between pulses). The lysate was centrifuged for 15 min at 12000 rpm, and the supernatant was collected for proteomic sample preparation. Protein concentrations were measured using a bicinchoninic acid (BCA) assay. An equal amount of proteins from PANC-1 and PANC-1R cells were mixed and followed by being reduced with 10 mM dithiothreitol (DTT) for 2 h at 37°C and alkylated with 20 mM iodoacetamide (IAA) for 30 min at room temperature in the dark. The remaining IAA was quenched by the addition of excess L-cysteine. Samples were diluted with 50 mM ammonium bicarbonate buffer to a final concentration of 1 M urea and then digested with trypsin (1:50, w/w) for 18 h at 37°C. To stop the digestion, 1% formic acid (FA) was added, and the resulting peptide mixtures were desalted with a 10 mg OASIS HLB cartridge (Waters, MA, USA). The eluted peptides were dried in a vacuum concentrator and reconstituted in 0.1% FA.

Liquid Chromatography-Tandem Mass Spectrometry (LC-MS/MS) Analysis

On-line 2D-nLC-MS/MS analysis was performed with a capillary LC system (Agilent Technologies, Waldbronn, Germany) coupled to a Q-Exactive™ hybrid quadrupole-Orbitrap mass spectrometer (Thermo Fisher Scientific). For on-line 2D-nLC, biphasic reverse phase (RP)/strong cation exchange (SCX) trap columns were packed in one-end tapered capillary tubing (360 μm-O.D., 200 μm-I.D., 40 mm in length) with 5 mm of C18 resin (5 μm-200 Å) followed by 15 mm of SCX resin (5 μm-200 Å), as previously described (16). The RP analytical column was packed in 150 mm capillary (360 μm-O.D., 75 μm-I.D.) with C18 resin (3 μm-100 Å).

The peptides were injected into the trap column and fractionated with 12-step salt gradients (0, 15, 20, 22.5, 25, 27.5, 30, 40, 50, 100, 200, and 1000 mM ammonium bicarbonate buffer containing 0.1% FA). The peptides eluted from SCX resin at each salt step were moved on to the RP resin of the trap column, followed by 120 min RP gradients at a column flow rate 200 nL/min. The mobile phase consisted of buffer A (0.1% FA in water) and B (2% water and 0.1% FA in acetonitrile). The gradient was 2% B for 10 min, 2–10% B for 1 min, 10-17% B for 4 min, 17–33% B for 70 min, 33–90% B for 3 min, 90% B for 15 min, and 90–2% B for 2 min and 2% B for 15 min.

The Q-Exactive mass spectrometer was operated in data-dependent mode. Full-scan MS spectra (*m/z* 300-1800) were acquired with automatic gain control (AGC) target value of 3E6 at a resolution of 70,000. MS/MS spectra were obtained at a resolution of 35,000. The top 12 most abundant ions from the MS scan were selected for high-energy collision dissociation (HCD) fragmentation with normalized collision energy (NCE) of 27%. Precursor ions with single and unassigned charge state were excluded. Dynamic exclusion was set to 30 s. Each biological replicate was analyzed in technical duplicate 2D LC runs.

Data Analysis

The MS raw data files were searched against the UniProt human database (Jan 3, 2018 release) using MaxQuant software (version 1.6.1.0) integrated with the Andromeda search engine for protein identification and SILAC quantification (17). The search criteria were set as follows: two mis-cleavages were allowed; the mass tolerance was 4.5 ppm and 20 ppm for precursor and fragment ions, respectively; carbamidomethylation of cysteine (C) was set as a fixed modification; oxidation of methionine (M) and acetylation of N-terminal residue was set as variable modifications; the false discovery rate (FDR) was set to 0.01 for both peptides

and proteins; SILAC heavy label was set to Arg6 and Lys8. Only proteins were identified with at least two unique peptides per protein. All contaminants and reverse database hits were excluded from the protein list. Subsequent data processing and statistical analysis were performed using the Perseus software 1.5.8.5 (18). The SILAC light/heavy ratios were $\log_2$ transformed and normalized by subtracting the median. To identify a significant difference between PANC-1 and PANC-1R cells, the Student's t-test was applied. A functional Gene Ontology (GO) enrichment analysis was performed using DAVID. The enrichment analysis of the reactome pathway was performed using the R/Bioconductor package ReactomePA (version 1.30.0) (19). A protein-protein interaction (PPI) network was constructed (high confidence score, > 0.7) with the Search Tool for the Retrieval of Interacting Genes/Proteins (STRING) 11.0 and then visualized using Cytoscape software 3.7.1. Network module analysis was performed using the Molecular Complex Deletion (MCODE) plugin for Cytoscape. The parameters were set as degree cut-off = 2, node score cutoff = 0.2, k-core = 2, and maximum depth = 100.

Western Blot Analysis

Harvested cells were lysed in cold radioimmunoprecipitation assay (RIPA) lysis buffer [0.5 M Tris-HCl (pH 7.4) 1.5 M NaCl, 2.5% deoxycholic acid, 10% NP-40, 10 mM EDTA] with protease and phosphatase inhibitors (Gendepot, Katy, TX, USA). Cell lysates were analyzed by sodium dodecyl sulfate-polyacrylamide gel electrophoresis (SDS-PAGE) and transferred to nitrocellulose membranes (GE Healthcare). After blocking with 8% skim milk or 5% bovine serum albumin (BSA) for 30 min, the membrane was probed with primary antibodies overnight at 4°C. After washing with phosphate-buffered saline (PBS)/1% Tween-20 (T-PBS), the membrane was developed with a peroxidase-conjugated secondary antibody from

Merck Millipore, and immunoreactive proteins were visualized using enhanced chemiluminescence reagents (Amersham Biosciences, Piscataway, NJ), as recommended by the manufacturer.

Primary antibodies were used for ISG15 (#2758), MARCKS (#5607), p-Akt (Ser473) (#9271), Akt (#9272), β-catenin (#9562), and cyclin D1 (#2978) from Cell Signaling Technology (CST, Beverly, MA). Primary antibodies were used for p53 (sc-126), IFIT3 (sc-393512), GAPDH (sc-47724), and HO-1 (sc-136960) from Santa Cruz Biotechnology (Santa Cruz, CA, USA). Anti-SOD2 (LF-PA0214) was obtained from Young In frontier (Seoul, Korea). Anti-β-actin (MAB1501) was obtained from Merck Millipore. Anti-WLS (655902 was obtained from Biolegend (San Diego, CA, USA).

RNA Isolation and qRT-PCR

Total RNA was purified using a TRIzol reagent (Ambion, Life Technologies, Carlsbad, CA, USA). 1ug of total RNA was synthesized to cDNA using a Prime Scrtipt™ 1st strand cDNA synthesis (TaKaRa, Japan). For analysis of relative quantitation, qRT-PCR reactions were subjected using TaKaRa SYBR Premix Ex Taq II (TaKaRa, Japan), and PCR processing was carried out in an iCycler (Bio-Rad, Hercules, CA). The sequences of primers for human *MARCKS* were 5'-CCAGTTCTCCAAGACCGCAG-3' (sense) and 5'-TCTCCTGTCCGT TCGCTTTG-3' (antisense). The sequences of primers for human *WLS* were 5'-GCACCAAGA AGCTGTGCATT-3' (sense) and 5'-GTTGTGGGCCCAATCAAGCC-3' (antisense). The sequences of primers for *GAPDH* were 5'-TCGACAGTCAGCCGCATCTTCTTT-3' (sense) and 5'-ACCAAATCCGTTGACTCCGACCTT-3' (antisense). The copy number of these genes was normalized to an endogenous reference gene, *GAPDH*. The fold change from PANC-1 was

set at 1-fold, and then the normalized fold change ratio was calculated. Data of relative gene expression was calculated by $2^{-\Delta\Delta CT}$ method (20).

siRNA Transfection

For knockdown of MARCKS or WLS, the transfection was performed with 20 nM siRNA using Lipofectamine 2000 (Invitrogen, Carlsbad, CA) according to the manufacturer's protocol. si-MARCKS (sc-35857) and si-WLS (sc-88713) were purchased from Santa Cruz Biotechnology (Santa Cruz, CA, USA).

Statistical analysis

All experiments were conducted in triplicate, and the mean values ± standard deviation (SD) values were presented. Comparisons between the two groups were considered using the Student's t-test. Differences between data groups were deemed statistically significant at $P < 0.05$.

Results

The Establishment and Validation of Oxaliplatin-Resistant PANC-1 cells

The human pancreatic cell line PANC-1 was subjected to gradually increasing concentrations of anticancer-drug. To examine the acquired drug resistance of PANC-1 cells, drug sensitivity to oxaliplatin was measured in parental and drug-resistant cells using a cell viability assay. The cell viability of parental PANC-1 cells was decreased depending on the concentration of oxaliplatin, whereas the oxaliplatin-resistant PANC-1 (PANC-1R) cells showed a high cell survival rate, even at high concentrations of oxaliplatin (Fig. 1A). To examine the potential of

tumorigenesis in oxaliplatin-resistant PANC-1R cells, we performed colony foramina assay. The colony-forming ability of PANC-1R cells was increased relative to the parental PANC-1 cells (Fig. 1B). These results indicate that PANC-1R cells exhibit the acquired chemoresistant features for oxaliplatin.

Quantitative Proteomic Analysis of Oxaliplatin Resistant and Sensitive PANC-1 Cells

To study changes in protein expression associated with oxaliplatin resistance in PANC-1 cells, SILAC-based quantitative proteomic analysis was performed using on-line 2D nLC-MS/MS. To this end, PANC-1 cells were metabolically labelled with two "heavy" isotope amino acids ($^{13}C_6$-Arg and $^{15}N_2{}^{13}C_6$-Lys), while PANC-1R cells were cultured with their "light" amino acid counterparts ($^{12}C_6$-Arg and $^{14}N_2{}^{12}C_6$-Lys) (Fig. 2A). Equal amount of PANC-1R (light) and PANC-1 (heavy) cell lysates were combined, followed by tryptic digestion and on-line 2D nLC-MS/MS analysis. Quality assessments of the proteomic dataset are shown in Figure 2B, and Supplemental Figure S1. There are linear correlations between biological replicates with *R* squared values ranging from 0.797 to 0.877 (Fig. 2B), indicating good reproducibility. Histograms of normalized $\log_2$ (light/heavy) were normally distributed (Supplemental Figure S1).

A total of 3544 proteins were commonly quantified in both PANC-1 and PANC-1R cells, considering only proteins that were quantified in at least three of the six replicates (Supplemental Table S1). Among these, 107 proteins were significantly changed between PANC-1 and PANC-1 R cells with thresholds of 2-fold changes and p-value 0.05 (Fig. 2C). Compared with oxaliplatin sensitive PANC-1 cells, 54 proteins were upregulated, and 53 proteins were downregulated in PANC-1R cells (Supplemental Tables S2 and S3). To gain more insight into the biological functions of significantly changed proteins, GO enrichment

297 analysis was performed using DAVID. All enriched GO terms, including biological processes
298 and molecular functions, are shown in Supplementary Table S4. The upregulated proteins
299 were mostly involved in base-excision repair (GO:0006284), cell-cell adhesion
300 (GO:0098609), and cellular response to the drug (GO:0035690), and the downregulated
301 proteins in type 1 interferon signalling pathway (GO:0060337), intrinsic apoptosis signalling
302 pathway in response to DNA damage (GO:0008630), and positive regulation of apoptotic
303 process (GO:0043065) (Fig. 2D). The reactome pathway analysis also revealed that
304 downregulated proteins were significantly enriched in interferon signalling, interferon-
305 alpha/beta signalling and DDX58/IFIH1-mediated induction of interferon-alpha/beta
306 signalling (Fig. 3). However, there was no significant enrichment of the reactome pathway
307 for upregulated proteins.

308 We further constructed the PPI network for 107 significantly changed proteins between
309 PANC-1 and PANC-1R cells using the STRING database and mapped with Cytoscape. After
310 excluding the disconnected proteins in the interaction networks (confidence score, > 0.7), 50
311 proteins were mapped in the PPI network (Fig. 4). Based on the MCODE analysis of PPI
312 network in Cytoscape, the most significant module (MCODE score = 9) consisted of nine
313 nodes (IFIT1, IFIT2, IFIT3, IFIH1, ISG15, OASL, DDX58, DDX60 and HERC5) with 36
314 edges, which were functionally associated with Type 1 interferon signalling pathway. Other
315 molecules were implicated in protein ubiquitination, neutrophil degranulation, and protein
316 hydroxylation (each MCODE score = 3).

317

318 **Verification of Differentially Expressed Proteins between Oxaliplatin Sensitive and**
319 **Resistant PANC-1 Cells by Western Blot.**

320 To verify quantitative proteomics datasets, Western blotting was performed for six

significantly changed proteins that are cellular tumour antigen p53 (p53), G2/mitotic-specific cyclin-B1 (Cyclin B1), superoxide dismutase (SOD2), interferon-induced protein with tetratricopeptide repeats 3 (IFIT3), ubiquitin-like protein ISG15 (ISG15), and heme oxygenase 1 (HO-1). From the Western blot assays, resultingly, the changes in expression levels – two (p53 and Cyclin B1) and four (SOD2, IFIT3, ISG15, and HO-1) proteins were upregulated and downregulated in PANC-1R cells, respectively, compared to those counterpart proteins in PANC-1 cells – were consistent with their quantitative proteomic results (Figs. 5A and B).

MARCKS or WLS was a Significant Factor for Chemoresistant in PANC-1R Cells

On the basis of upregulated proteins in PANC-1R cells, we hypothesized that fundamental factors, which is highly expressed in PANC-1R cells, can induce tolerance to oxaliplatin in cancer cells. MARCKS was highly expressed in PANC-1 R cells (Supplemental Table S2). MARCKS is involved in transducing receptor-mediated signals into intracellular kinases, such as Akt and PKC (21-23). The SILAC ratio of MARCKS protein expression level was 6-fold higher in PANC-1R cells compared to PANC-1 cells (Fig. 6A). The mRNA level of MARCKS measured by qRT-PCR was also 6-fold higher in PANC-1R cells compared to PANC-1 cells (Fig. 6B). To confirm the protein level and activity of MARKCS, we examined the levels of MARCKS and its downstream protein using Western blot analysis. We found that the protein levels of MARCK and AKT phosphorylation were increased in PANC-1 R cells (Fig. 6C).

Wntless homolog protein (WLS, Evi or GPR177) was also detected to be highly expressed in PANC-1R cells (Supplemental Table S2), and WLS regulates the sorting and secretion of wnt proteins (24). The SILAC ratio of WLS protein expression level was 4-fold

higher in PANC-1R cells compared to PANC-1 cells (Fig. 6D). The mRNA level of WLS is also elevated in PANC-1R cells (Fig. 6E). WLS is essential for β-catenin signalling (25, 26). To check the activity of WLS, we examined the level of β-catenin and its target cyclin D1 (27, 28). Up-regulation of WLS in PANC-1R cells increased the expression of β-catenin and cyclin D1 (Fig. 6F).

Inhibition of MARCKS and WLS Increased Oxaliplatin-mediated Cell Death in Chemoresistant PANC-1R Cells

Next, we explored whether down-regulation of MARCKS and WLS in PANC-1R cells affects cell survival for oxaliplatin treatment. When silencing in PANC-1R cells using siRNA specific for MARCKS or WLS, cell viability to oxaliplatin was slightly decreased compared to PANC-1R control cells (siCon) (Figs. 7A and B). However, when silencing both MARCKS and WLS at the same time, the decrease in cell viability was significantly reduced compared to single gene silencing (Figs. 7C and D). These results indicated that drug resistance in PANC-1 R cells was regulated by the association of several factors rather than by a single factor.

Discussion

To understand the mechanism of oxaliplatin resistant in pancreatic cancer cells, we successfully established oxaliplatin resistant pancreatic cancer PNAC-1 cell lines by a stepwise increase of oxaliplatin concentration in a culture medium. Using SILAC-based 2D-nLC-MS/MS, the quantitative proteomic analysis was performed across PANC-1R and PANC-1 cells. We identified a number of significantly changed proteins in oxaliplatin resistant cells compared with sensitive cells, which were associated to multiple biological

processes, including DNA repair system, cellular response to drug, apoptotic signalling and type 1 interferon signalling pathway.

We identified the up-regulation of base-excision repair in PANC-1R cells compared to PANC-1 cells (Fig. 2D and Supplemental Table S3). Base-excision repair is one of the major DNA repair systems for oxidative DNA damages, which is a known pathway involved in resistance to oxaliplatin (12, 29). Because oxaliplatin induces the formation of free radicals as well as oxaliplatin-DNA adducts, exposure to oxaliplatin causes oxidative DNA damages and subsequently cytotoxicity (10, 30). Therefore, an increase of base-excision repair capacity could contribute the resistance to oxaliplatin-induced cytotoxicity. In agreement with this, the down-regulation of the apoptotic pathway in response to DNA damage was identified in PANC-1R cells (Fig. 2D and Supplemental Table S3).

Our study also identified type 1 interferon signalling-related proteins (IFIT1, IFIT2, IFIT3, OASL and ISG15) that were down-regulated in PANC-1R cells (Figs. 2D and 3), and further confirmed the expression level of IFIT3 and ISG15 by Western blot (Fig. 5B). So far, little is known about the role of type 1 interferon signalling in resistance to platinum drugs. Huo et al. reported that silencing of ISG15 increased cisplatin resistance in colorectal cancer A549 cells by the increase of p53 stability (31), which is consistent with our findings of a down-regulation of ISG15 and up-regulation of p53 in PANC-1R cells. In contrast, another study has shown that the activation of the STAT1 pathway and downstream interferon-stimulated genes contributes to platinum drug resistance in human ovarian cancer cells (32).

It is notable that the expression of MARCKS was upregulated at both the mRNA and protein levels in PANC-1 R cells (Figs. 6A-C). MARCKS is a substrate of protein kinase C that plays a regulatory role in various cellular functions, such as actin cytoskeleton, cell migration, and cell cycles (23), which had not been previously identified to be involved in

393 oxaliplatin resistance. Recent studies have shown that MARCKS regulates intracellular
394 phosphatidylinositol 4, 5-bisphosphate (PIP2) levels and thereby activating PI3K/AKT
395 signalling (33-35). In addition, MARCKS knockdown reduces phosphorylation of PI3K and
396 AKT in non-small-cell lung cancer (NSCLC) cells (36) and renal cell carcinoma (RCC) (21).
397 In the present study, we show an increase in the levels of AKT phosphorylation (Ser473 and
398 Thr308) in PANC-1R cells. (Fig. 6C). Since activation of the PI3K/AKT signalling pathway
399 contributes to oxaliplatin resistance in hepatocellular carcinoma (37), colon cancer (38), and
400 cholangiocarcinoma cells (39), it is possible that oxaliplatin resistance was acquired by
401 activation of MARCKS and its downstream AKT signalling in pancreatic cancer cells.
402 WLS is a transmembrane protein that regulates tracking and secretion of Wnt
403 signalling molecules (40). Secreted Wnt ligands bind to Frizzled receptors and LRP 5/6 co-
404 receptors, resulting in the activation of Wnt/β-catenin signalling pathway (40, 41). Wnt/β-
405 catenin signalling plays an important role in the cellular and developmental process and is
406 aberrantly activated in various types of cancer (41-43). Several previous studies demonstrated
407 the association of the Wnt/β-catenin pathway with chemoresistance in cancer cells (44-46).
408 Kukcinaviciute et al. have reported the up-regulation of the Wnt pathway in oxaliplatin-
409 resistance colorectal cancer cells HCT116 (44). Our proteomic results have shown the up-
410 regulation of WLS in PANC-1 R cells, and it was confirmed by qRT-PCR and Western blot
411 (Figs. 6D-F). We also observed the overexpression of β-catenin and its target gene cyclin D1
412 in PANC-1R cells by Western blot (Fig. 6F), which indicates the activation of the Wnt/β-
413 catenin pathway in oxaliplatin resistant cells, compared to sensitive cells. These results
414 suggested that activation of Wnt/β-catenin signalling might lead to oxaliplatin resistance in
415 pancreatic cancer cells. Furthermore, we demonstrated that dual suppression of MARCKS
416 and WLS showed a synergistic effect on increasing oxaliplatin sensitivity of PANC-1 R cells

(Fig. 7).

In conclusion, the present study revealed the multifactorial mechanisms involved in oxaliplatin resistance in pancreatic cancer cells by performing a SILAC-based quantitative proteomic profiling. Moreover, functional studies demonstrated that up-regulation of MARCKS (Akt signalling) and WLS (Wnt/β-catenin signalling) contributes to the oxaliplatin resistance (Fig. 8). Further investigation is required to elucidate detailed mechanisms, which will help to develop new therapeutic strategies for overcoming oxaliplatin resistance in the treatment of pancreatic cancer.

Author contributions

H.H.J. and D.K. designed the study. D.K. and H.H.J. wrote the manuscript with help from all authors. E.-K.K. and M.-J.S. performed the cell culture and biological validation experiments under the supervision of H.H.J. Y.E.K. performed proteomic experiments and bioinformatics analysis under the supervision of T.-Y.K. and D.K.

Acknowledgements

This research was supported by the Technology Innovation Program (20009350, Establishment of the measurement standards for toxicity and drug metabolism based on human stem cell-derived organoid models) funded by the Ministry of Trade, Industry & Energy (MOTIE, Korea). This research was also supported, in part, by a project of the Korea Research Institute of Standards and Science (KRISS) under the project title ″Establishment for Metrology in Bioanalysis″ (GP2020-0003-05).

Conflicts of interest

The authors declare no conflicts of interest.

Data availability

Excel file containing the analyzed data are provided in Supplementary Information. The datasets generated via nLC-ESI-MS/MS analyses in this study are available in PRIDE, accession number: PXD021251. https://www.ebi.ac.uk/pride.

References

1. Siegel, R. L., Miller, K. D., and Jemal, A. (2018) Cancer statistics, 2018. *CA Cancer J Clin* 68, 7-30

2. Paul, E. O., and Kenneth, P. O. (2013) Pancreatic cancer: why is it so hard to treat? *Therap Adv Gastroenterol* 6, 321–337

3. Sheikh, R., Walsh, N., Clynes, M., O'Connor, R., and McDermott, R. (2010) Challenges of drug resistance in the management of pancreatic cancer. *Expert Rev Anticancer Ther* 10, 1647-1661

4. Comella, P., Casaretti, R., Sandomenico, C., Avallone, A., and Franco, L. (2009) Role of oxaliplatin in the treatment of colorectal cancer. *Ther Clin Risk Manag* 5, 229-238

5. Inadomi, K., Kusaba, H., Matsushita, Y., Tanaka, R., Mitsugi, K., Arimizu, K., Hirano, G., Makiyama, A., Ohmura, H., Uchino, K., Hanamura, F., Shibata, Y., Kuwayama, M., Esaki, T., Takayoshi, K., Arita, S., Ariyama, H., Akashi, K., and Baba, E. (2017) Efficacy and Safety Analysis of Oxaliplatin-based Chemotherapy for Advanced Gastric Cancer. *Anticancer Res* 37, 2663-2671

6. Neoptolemos, J. P., Kleeff, J., Michl, P., Costello, E., Greenhalf, W., and Palmer, D. H. (2018) Therapeutic developments in pancreatic cancer: current and future perspectives. *Nat Rev Gastroenterol Hepatol* 15, 333-348

463 7. Saung, M. T., and Zheng, L. (2017) Current Standards of Chemotherapy for Pancreatic Cancer.
464 *Clin Ther* 39, 2125-2134
465 8. Alcindor, T., and Beauger, N. (2011) Oxaliplatin: a review in the era of molecularly targeted
466 therapy. *Curr Oncol* 18, 18-25
467 9. Seetharam, R., Sood, A., and Goel, S. (2009) Oxaliplatin: pre-clinical perspectives on the
468 mechanisms of action, response and resistance. *Ecancermedicalscience* 3, 153
469 10. Martinez-Balibrea, E., Martinez-Cardus, A., Gines, A., Ruiz de Porras, V., Moutinho, C.,
470 Layos, L., Manzano, J. L., Buges, C., Bystrup, S., Esteller, M., and Abad, A. (2015) Tumor-Related
471 Molecular Mechanisms of Oxaliplatin Resistance. *Mol Cancer Ther* 14, 1767-1776
472 11. Rakitina, T. V., Vasilevskaya, I. A., and O'Dwyer, P. J. (2003) Additive interaction of
473 oxaliplatin and 17-allylamino-17-demethoxygeldanamycin in colon cancer cell lines results from
474 inhibition of nuclear factor kappaB signaling. *Cancer Res* 63, 8600-8605
475 12. Martin, L. P., Hamilton, T. C., and Schilder, R. J. (2008) Platinum resistance: the role of DNA
476 repair pathways. *Clin Cancer Res* 14, 1291-1295
477 13. Li, X. H., Li, C., and Xiao, Z. Q. (2011) Proteomics for identifying mechanisms and
478 biomarkers of drug resistance in cancer. *J Proteomics* 74, 2642-2649
479 14. An, Y., Zhou, L., Huang, Z., Nice, E. C., Zhang, H., and Huang, C. (2019) Molecular insights
480 into cancer drug resistance from a proteomics perspective. *Expert Rev Proteomics* 16, 413-429
481 15. Martinez-Balibrea, E., Plasencia, C., Gines, A., Martinez-Cardus, A., Musulen, E., Aguilera,
482 R., Manzano, J. L., Neamati, N., and Abad, A. (2009) A proteomic approach links decreased pyruvate
483 kinase M2 expression to oxaliplatin resistance in patients with colorectal cancer and in human cell lines.
484 *Mol Cancer Ther* 8, 771-778
485 16. Kang, D., Nam, H., Kim, Y. S., and Moon, M. H. (2005) Dual-purpose sample trap for on-line
486 strong cation-exchange chromatography/reversed-phase liquid chromatography/tandem mass
487 spectrometry for shotgun proteomics. Application to the human Jurkat T-cell proteome. *J Chromatogr*
488 *A* 1070, 193-200

17. Cox, J., and Mann, M. (2008) MaxQuant enables high peptide identification rates, individualized p.p.b.-range mass accuracies and proteome-wide protein quantification. *Nat Biotechnol* 26, 1367-1372

18. Tyanova, S., Temu, T., Sinitcyn, P., Carlson, A., Hein, M. Y., Geiger, T., Mann, M., and Cox, J. (2016) The Perseus computational platform for comprehensive analysis of (prote)omics data. *Nat Methods* 13, 731-740

19. Yu, G., and He, Q. Y. (2016) ReactomePA: an R/Bioconductor package for reactome pathway analysis and visualization. *Mol Biosyst* 12, 477-479

20. Livak, K. J., and Schmittgen, T. D. (2001) Analysis of relative gene expression data using real-time quantitative PCR and the 2(-Delta Delta C(T)) Method. *Methods* 25, 402-408

21. Chen, C. H., Fong, L. W. R., Yu, E., Wu, R., Trott, J. F., and Weiss, R. H. (2017) Upregulation of MARCKS in kidney cancer and its potential as a therapeutic target. *Oncogene* 36, 3588-3598

22. Chen, C. H., Thai, P., Yoneda, K., Adler, K. B., Yang, P. C., and Wu, R. (2014) A peptide that inhibits function of Myristoylated Alanine-Rich C Kinase Substrate (MARCKS) reduces lung cancer metastasis. *Oncogene* 33, 3696-3706

23. Fong, L. W. R., Yang, D. C., and Chen, C. H. (2017) Myristoylated alanine-rich C kinase substrate (MARCKS): a multirole signaling protein in cancers. *Cancer Metastasis Rev* 36, 737-747

24. Glaeser, K., Urban, M., Fenech, E., Voloshanenko, O., Kranz, D., Lari, F., Christianson, J. C., and Boutros, M. (2018) ERAD-dependent control of the Wnt secretory factor Evi. *EMBO J* 37

25. Yang, P. T., Anastas, J. N., Toroni, R. A., Shinohara, M. M., Goodson, J. M., Bosserhoff, A. K., Chien, A. J., and Moon, R. T. (2012) WLS inhibits melanoma cell proliferation through the beta-catenin signalling pathway and induces spontaneous metastasis. *EMBO Mol Med* 4, 1294-1307

26. Adell, T., Salo, E., Boutros, M., and Bartscherer, K. (2009) Smed-Evi/Wntless is required for beta-catenin-dependent and -independent processes during planarian regeneration. *Development* 136, 905-910

27. Vlad-Fiegen, A., Langerak, A., Eberth, S., and Muller, O. (2012) The Wnt pathway destabilizes

515 adherens junctions and promotes cell migration via beta-catenin and its target gene cyclin D1. *FEBS*
516 *Open Bio* 2, 26-31
517 28. Shtutman, M., Zhurinsky, J., Simcha, I., Albanese, C., D'Amico, M., Pestell, R., and Ben-Ze'ev,
518 A. (1999) The cyclin D1 gene is a target of the beta-catenin/LEF-1 pathway. *Proc Natl Acad Sci U S A*
519 96, 5522-5527
520 29. Manic, S., Gatti, L., Carenini, N., Fumagalli, G., Zunino, F., and Perego, P. (2003) Mechanisms
521 controlling sensitivity to platinum complexes: role of p53 and DNA mismatch repair. *Curr Cancer Drug*
522 *Targets* 3, 21-29
523 30. Srinivas, U. S., Tan, B. W. Q., Vellayappan, B. A., and Jeyasekharan, A. D. (2019) ROS and
524 the DNA damage response in cancer. *Redox Biol* 25, 101084
525 31. Huo, Y., Zong, Z., Wang, Q., Zhang, Z., and Deng, H. (2017) ISG15 silencing increases
526 cisplatin resistance via activating p53-mediated cell DNA repair. *Oncotarget* 8, 107452-107461
527 32. Roberts, D., Schick, J., Conway, S., Biade, S., Laub, P. B., Stevenson, J. P., Hamilton, T. C.,
528 O'Dwyer, P. J., and Johnson, S. W. (2005) Identification of genes associated with platinum drug
529 sensitivity and resistance in human ovarian cancer cells. *Br J Cancer* 92, 1149-1158
530 33. Chen, C. H., Statt, S., Chiu, C. L., Thai, P., Arif, M., Adler, K. B., and Wu, R. (2014) Targeting
531 myristoylated alanine-rich C kinase substrate phosphorylation site domain in lung cancer. Mechanisms
532 and therapeutic implications. *Am J Respir Crit Care Med* 190, 1127-1138
533 34. Hanada, S., Kakehashi, A., Nishiyama, N., Wei, M., Yamano, S., Chung, K., Komatsu, H.,
534 Inoue, H., Suehiro, S., and Wanibuchi, H. (2013) Myristoylated alanine-rich C-kinase substrate as a
535 prognostic biomarker in human primary lung squamous cell carcinoma. *Cancer Biomark* 13, 289-298
536 35. Ziemba, B., Burke, J., Masson, G., Williams, R., and Falke, J. (2016) Regulation of PI3K by
537 PKC and MARCKS: Single-Molecule Analysis of a Reconstituted Signaling Pathway. *Biophys J* 110,
538 1811-1825
539 36. Chen, C. H., Thai, P., Yoneda, K., Adler, K. B., Yang, P. C., and Wu, R. (2014) A peptide that
540 inhibits function of Myristoylated Alanine-Rich C Kinase Substrate (MARCKS) reduces lung cancer

541 metastasis. *Oncogene* 33, 3696-3706

542 37. Xiu, P., Dong, X., Dong, X., Xu, Z., Zhu, H., Liu, F., Wei, Z., Zhai, B., Kanwar, J. R., Jiang,
543 H., Li, J., and Sun, X. (2013) Secretory clusterin contributes to oxaliplatin resistance by activating Akt
544 pathway in hepatocellular carcinoma. *Cancer Sci* 104, 375-382

545 38. Chen, J., Huang, X. F., Qiao, L., and Katsifis, A. (2011) Insulin caused drug resistance to
546 oxaliplatin in colon cancer cell line HT29. *J Gastrointest Oncol* 2, 27-33

547 39. Leelawat, K., Narong, S., Udomchaiprasertkul, W., Leelawat, S., and Tungpradubkul, S. (2009)
548 Inhibition of PI3K increases oxaliplatin sensitivity in cholangiocarcinoma cells. *Cancer Cell Int* 9, 3

549 40. Das, S., Yu, S., Sakamori, R., Stypulkowski, E., and Gao, N. (2012) Wntless in Wnt secretion:
550 molecular, cellular and genetic aspects. *Front Biol (Beijing)* 7, 587-593

551 41. Zhan, T., Rindtorff, N., and Boutros, M. (2017) Wnt signaling in cancer. *Oncogene* 36, 1461-
552 1473

553 42. Polakis, P. (2007) The many ways of Wnt in cancer. *Curr Opin Genet Dev* 17, 45-51

554 43. Barker, N., and Clevers, H. (2006) Mining the Wnt pathway for cancer therapeutics. *Nat Rev*
555 *Drug Discov* 5, 997-1014

556 44. Kukcinaviciute, E., Jonusiene, V., Sasnauskiene, A., Dabkeviciene, D., Eidenaite, E., and
557 Laurinavicius, A. (2018) Significance of Notch and Wnt signaling for chemoresistance of colorectal
558 cancer cells HCT116. *J Cell Biochem* 119, 5913-5920

559 45. Chikazawa, N., Tanaka, H., Tasaka, T., Nakamura, M., Tanaka, M., Onishi, H., and Katano, M.
560 (2010) Inhibition of Wnt signaling pathway decreases chemotherapy-resistant side-population colon
561 cancer cells. *Anticancer Res* 30, 2041-2048

562 46. Cui, J., Jiang, W., Wang, S., Wang, L., and Xie, K. (2012) Role of Wnt/beta-catenin signaling
563 in drug resistance of pancreatic cancer. *Curr Pharm Des* 18, 2464-2471

564

565

566 # Figures and Figure legends

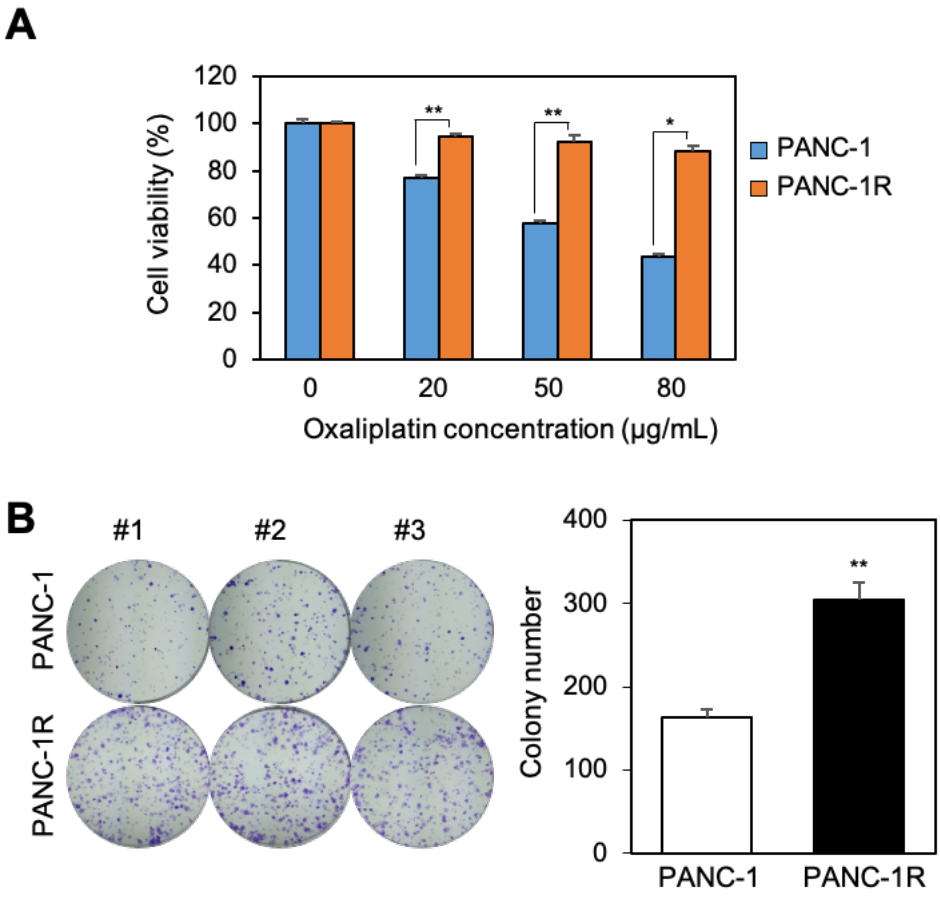

567

568 **Figure 1. Establishment of oxaliplatin-resistant pancreatic cancer cell line.** (A) Cellular
569 viability was assayed by Ez-cytox on PANC-1 and PANC-1R with oxaliplatin for 2 days. (B)
570 The colony formation assays were performed on PANC-1 and PANC-1R, respectively.
571 Representative pictures for the formation of the colony are shown. Counting of colony
572 numbers is shown. Three independent experiments were performed in triplicates. *$p < 0.05$,
573 **$p < 0.01$.

574

575

576

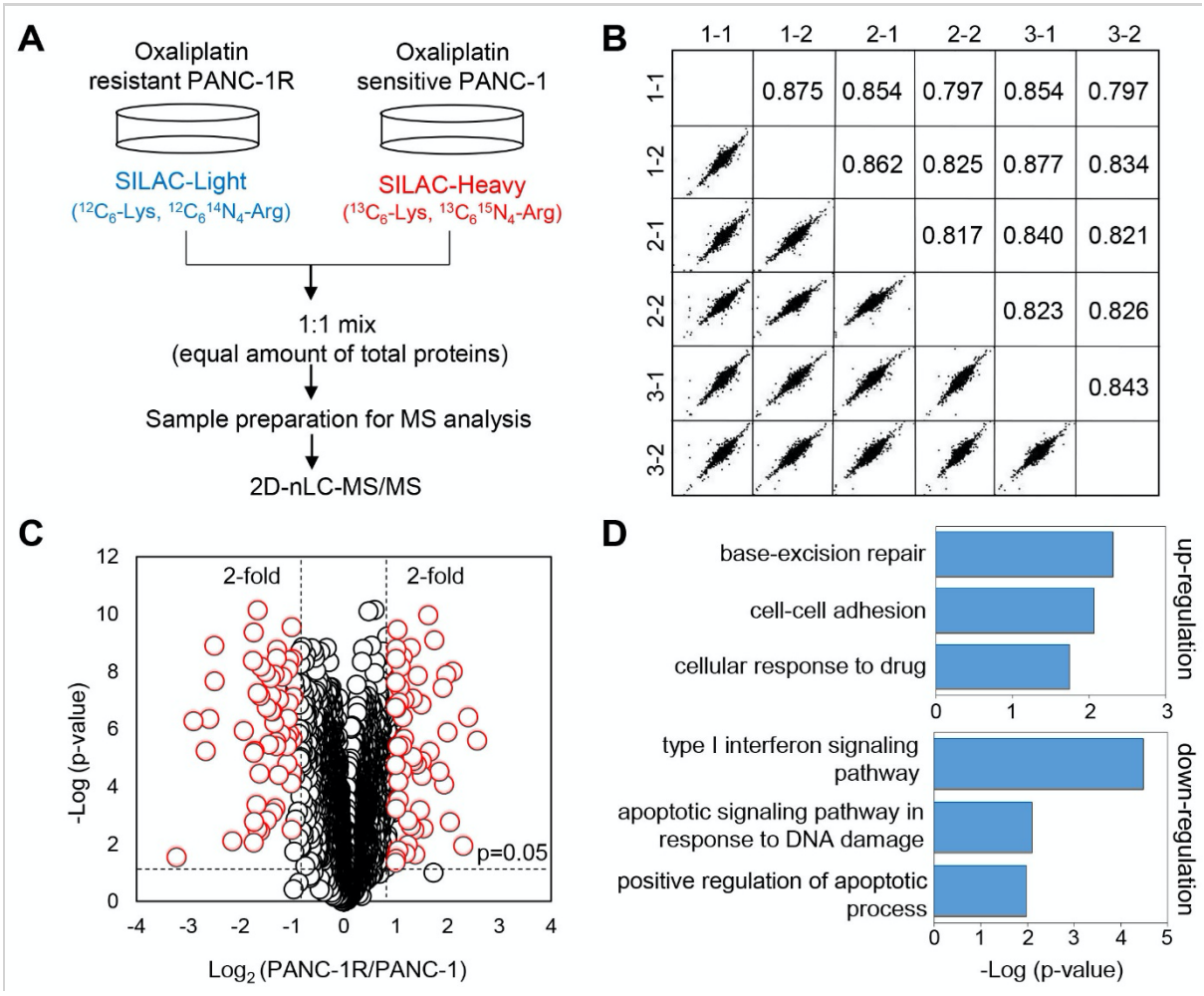

Figure 2. Proteomic comparison of oxaliplatin sensitive and resistant PANC-1 cells. (A) Proteomic workflow for SILAC labeling and LC-MS/MS (B) Multiple scatter plots demonstrating reproducibility between the biological and technical replicates. Represented values are Pearson correlation coefficients. (C) Volcano plot showing the $\log_2$ fold-change and significance ($-\log_{10}$ p-value) of the proteome dataset. The cut-off values of fold-changes and significance is indicated with a dashed line. Red dots represent significantly changed proteins according to the p-value and fold-change cut-off values. (D) DAVID Gene Ontology enrichment analysis of up-/down-regulated proteins by biological process. PANC-1R, oxaliplatin resistant PANC-1 cells.

588

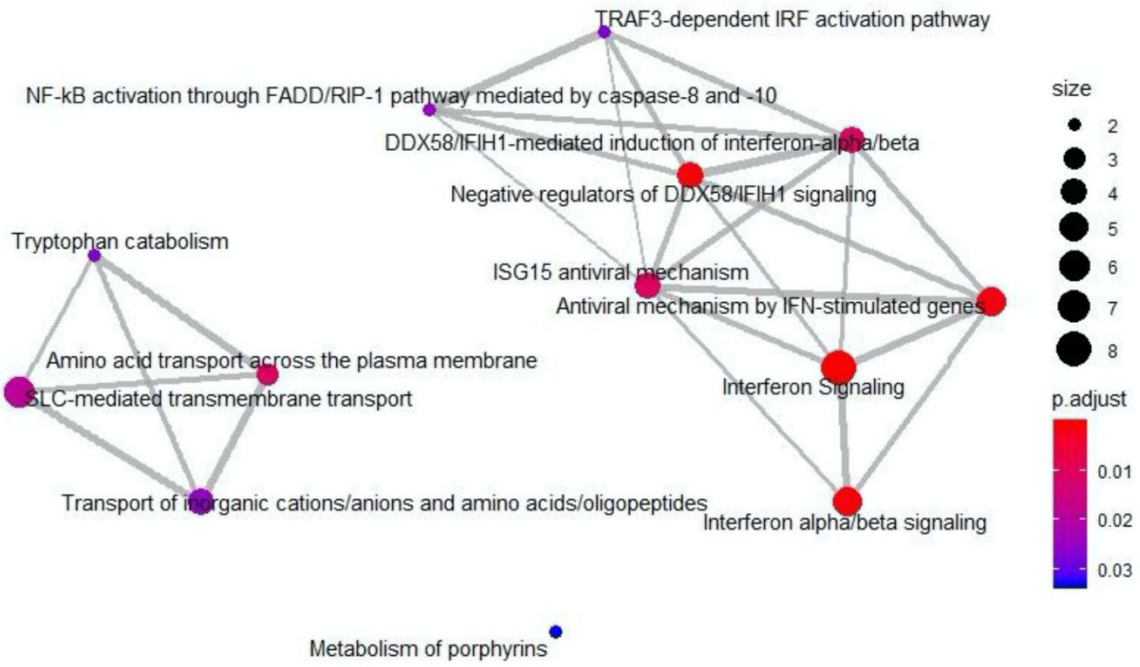

589

590

591 **Figure 3. Reactome pathway enrichment map for down-regulated proteins in oxaliplatin**

592 **resistant PANC-1 cells**. The node color indicates significance of the reactome pathway and

593 the node size represents the number of genes in the reactome pathway.

594

595

596

597

598

599

600

601

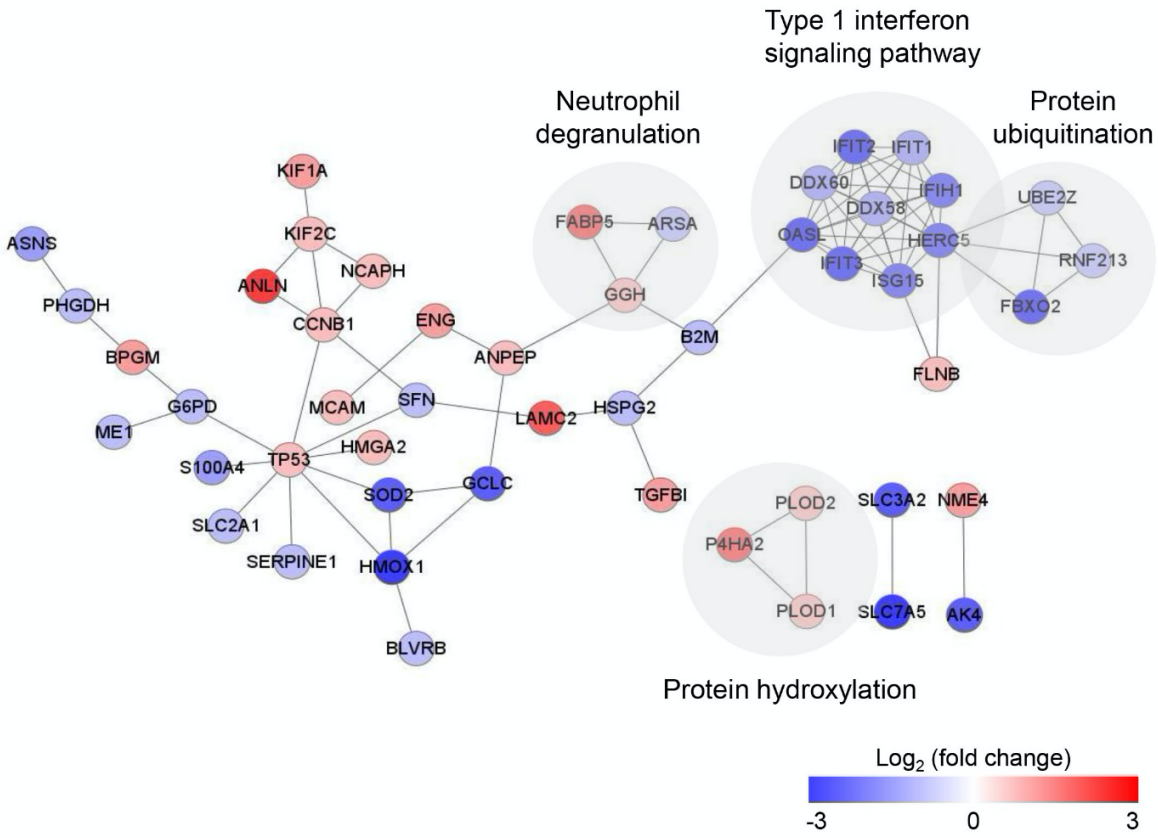

Figure 4. Protein-protein interaction (PPI) analysis of significantly changed proteins in oxaliplatin resistant PANC-1 cells. The network was mapped using the STRING database and visualized by Cytoscape 3.7.2. Red nodes indicate up-regulation and blue nodes indicate down-regulation.

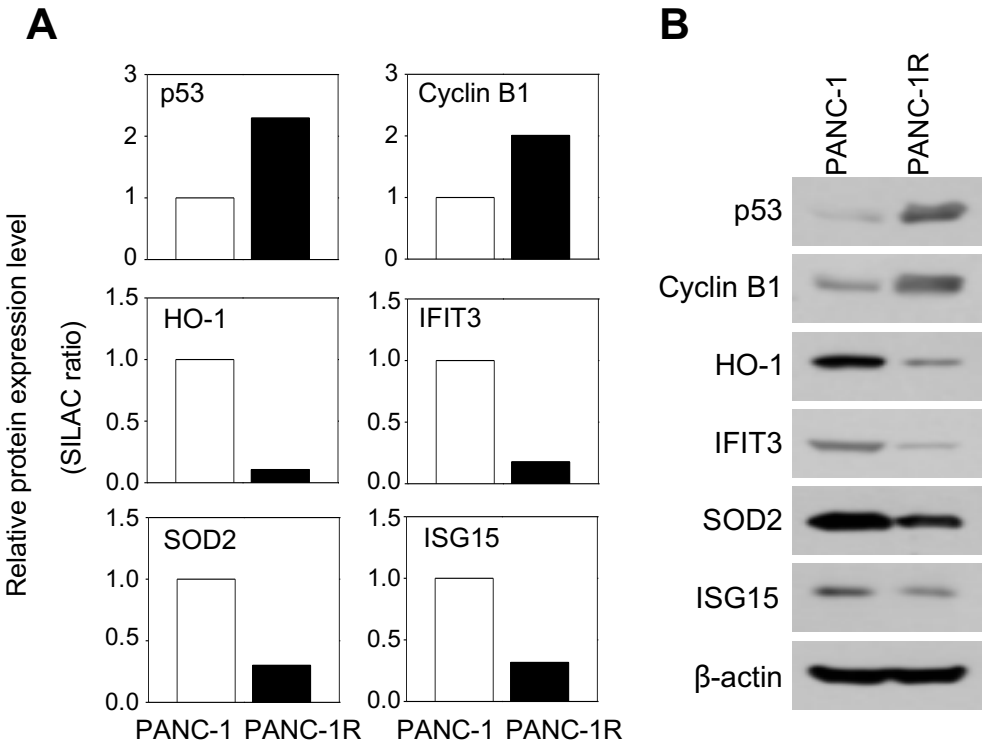

Figure 5. Validation of SILAC data by Western blot analysis. (A) Relative protein expression level of selected proteins (p53, Cyclin B1, SOD2, IFIT3, ISG15 and HO-1) from SILAC data. Protein expression levels were normalized to oxaliplatin sensitive PANC-1 cells. (B) Validation of selected proteins (p53, Cyclin B1, SOD2, IFIT3, ISG15 and HO-1) in both oxaliplatin sensitive and resistant PANC-1 cells by Western blot. ACTB was used as a loading control.

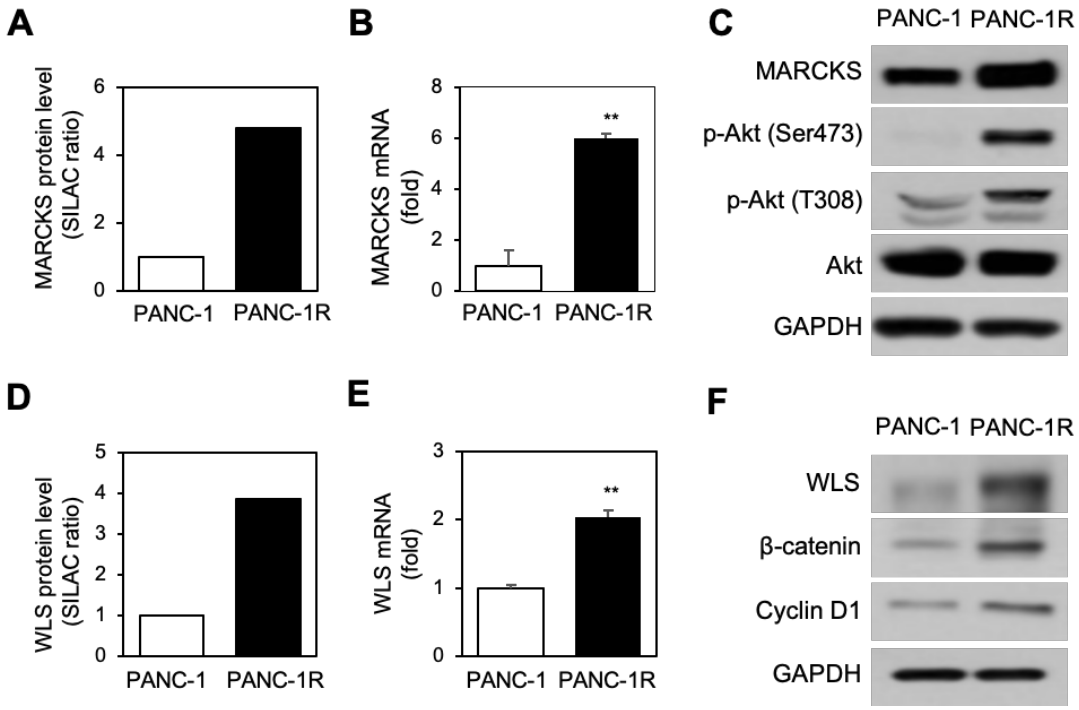

Figure 6. MARCKS- or WLS-mediated downstream signaling is activated in PANC-1R cells. (A) The SILAC ratio of MARCKS was increased in PANC-1R cells. (B) The quantitative level of MARCKS mRNA by qRT-PCR was higher in PANC-1R cells. Three independent experiments were performed in triplicates. (C) The protein level of MARCKS, phosphor-Akt (Ser473 or Thr308), and total Akt was determined by Western blotting. GAPDH was the loading control. (D) The SILAC ratio of WLS was increased in PANC-1R cells. (E) The level of WLS mRNA by qRT-PCR was higher in PANC-1R cells. Three independent experiments were performed in triplicate. (F) The protein level of WLS, β-catenin, and cyclin D1 was determined by Western blotting. GAPDH was loading control. $^{**}p < 0.01$.

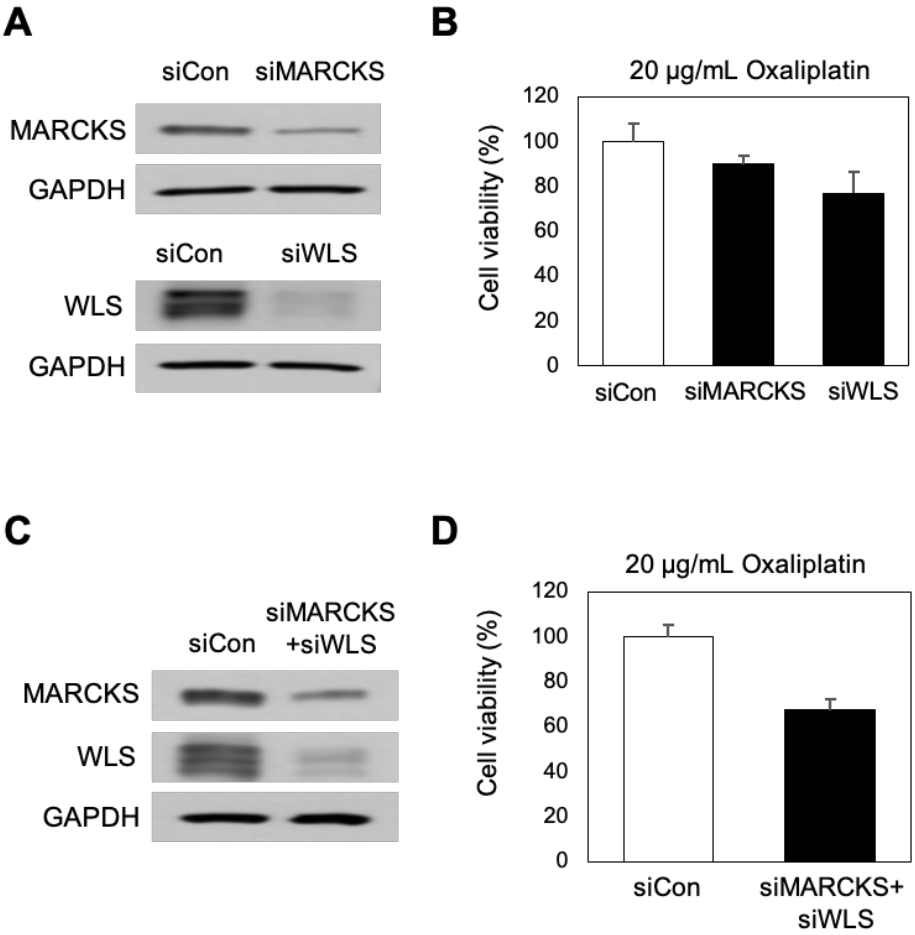

Figure 7. The inhibition of MARCKS and WLS induced PANC-1R cells to be sensitive to oxaliplatin. (A) The level of MARCKS or WLS in PANC-1R cell with the treatment of siMARCKS or siWLS was obtained by Western blotting. (B) The cell viability to oxaliplatin was analyzed by Ex-cytox in PANC-1R with knockdown of MARCKS or WLS. (C) The levels of MARCKS and WLS in PANC-1R cells treated with both siMARCKS and siWLS were obtained by Western blotting. (D) The cell viability to oxaliplatin was analyzed by Ex-cytox in PANC-1R cells treated with both siMARCKS and siWLS. $^{**}p < 0.01$.

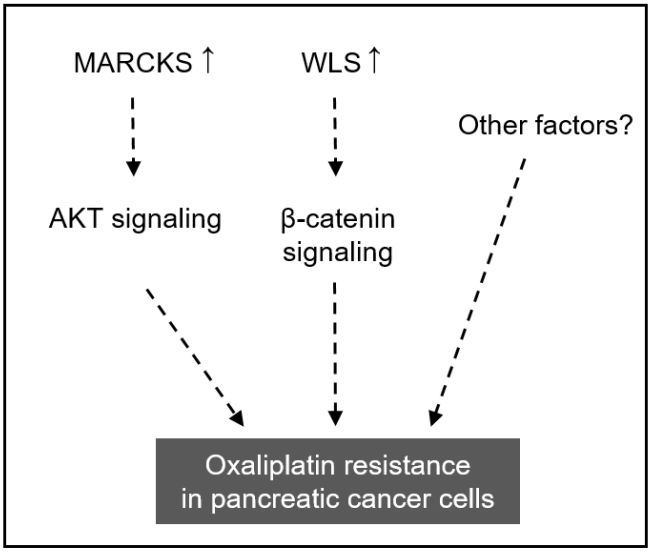

Figure 8. Schematic model of oxaliplatin resistance in pancreatic cancer cells